Direct Determination of Wind Shears from the Gradients of Satellite Radiance Observations

GEORGE OHRING

Department of Geophysics and Planetary Sciences, Tel Aviv University, Ramat Aviv, Israel, and Earth Sciences Laboratory, NESS, NOAA, Washington, DC 20233

BINYAMIN NEEMAN

Department of Geophysics and Planetary Sciences, Tel Aviv University, Ramat Aviv, Israel

LOUIS D. DUNCAN

Atmospheric Sciences Laboratory, White Sands Missile Range, NM 88002

(Manuscript received 9 March 1981, in final form 11 July 1981)

ABSTRACT

To the extent that the stratospheric wind field is close to geostrophic, the thermal wind is a good approximation to the vertical wind shear (vertical variation of the horizontal wind). And since the thermal wind is proportional to the horizontal temperature gradient, the possibility exists of determining it from satellite radiance observations. Several different methods are developed here for retrieving thermal winds directly from the horizontal gradients of satellite radiance observations, without first retrieving the horizontal temperature gradient. The methods are applied to the determination of thermal winds in the upper troposphere and lower stratosphere over the White Sands Missile Range area. A special series of about 30 concurrent sets of radiance observations from the NOAA-4 VTPR instrument and wind shears from radiosonde observations (for ground truth) distributed throughout one year, is used for these tests. The results obtained with these direct methods are compared with results obtained with 1) a traditional method, in which temperature profiles are first retrieved from the satellite radiances and the thermal winds are then obtained from the horizontal gradients of the retrieved temperatures; and 2) a linear regression between observed radiance gradients and observed wind shears. The latter method serves as an estimate of the upper limit of accuracy to be obtained by any method based on a linear combination of radiance gradients.

The results indicate that the direct methods may be divided into two groups, with much better retrievals for one of these groups. The probable reasons for these differences are identified. The best direct methods yield results comparable to the traditional method. In comparison with ground truth none of the methods is particularly skillful. The lack of skill in these particular cases is attributed mainly to the modest wind shears contained in the sample. Errors associated with trying to measure relatively small horizontal radiance gradients over relatively small horizontal distances result in residual uncertainty nearly as large as the variance of the sample. It is suggested that much better results would be obtained if some of the better methods were to be applied over greater horizontal distances or to regions with larger wind shears.

1. Introduction

Satellite radiance observations have been used for some time now to infer atmospheric temperatures. The concept of using satellite-observed radiances to infer atmospheric wind shears (vertical variations of the horizontal wind) is based on the following physical principles:

(i) The satellite observed spectrum of radiance above a particular point on the earth's surface depends on the vertical temperature profile above that point.

(ii) The wind shear in a layer is directly related to the horizontal gradient of the mean temperature of that layer (through the thermal wind equation) to the extent that the wind is geostrophic—as it generally is, to a good approximation, above the planetary boundary layer outside the tropics.

From (i) and (ii), one should be able, in principle, to estimate the wind shears directly from the horizontal gradients of satellite-observed radiances. Because of the inherent vertical resolution of the satellite-observed temperature profile, layer-mean temperatures should be more accurate than temperatures at specific levels. Since it is the gradient of layer-mean temperature that is involved in the thermal wind equation, satellite radiance observations should be particularly appropriate for this purpose.

Some attempts along these lines have already been made. For example, Zak and Panofsky (1968)

0021-8952/81/111336-08$06.00

used a regression technique to relate 10 mb geostrophic winds to "thermal winds" obtained from the horizontal gradients of blackbody temperatures based on broad-band 15 μm satellite radiance observations. Grody *et al.* (1979) used the radial gradients of satellite-observed microwave brightness temperatures at 55.45 GHz to estimate the 700 mb wind field across a typhoon.

In the present study, we develop and test several methods for retrieving atmospheric wind shears directly from satellite-observed radiance gradients. The methods are applied to the determination of stratospheric wind shears from the horizontal gradients of NOAA-4 VTPR observations over the White Sands Proving Ground, New Mexico, where a special series of radiosonde observations provided "ground truth". The radiance observations were used at their full resolution. Stratospheric (rather than tropospheric) wind shears are emphasized in order to eliminate the effects on the radiances of surface boundary terms and to minimize the effects of possible cloud contamination. These direct methods are intercompared and then compared with results obtained with the "traditional" methods in which the wind shear is computed from the temperatures retrieved from the radiance observations, and with a linear regression method based on the relationship between observed wind shears and observed radiance gradients.

2. Derivation of retrieval methods

The satellite-observed radiance for an observing wavenumber with negligible contribution from the earth's surface may be written as

$$R_i = \int_0^{Z_T} B_i \frac{d\tau_i}{dZ}\, dZ, \tag{1}$$

where i is an index for observing wavenumber, B the Planck function, τ the transmittance from the level Z to the top of the radiating atmosphere, Z_T, and Z a measure of the altitude in terms of scale heights, i.e.,

$$Z = -\ln(p/p_0), \tag{2}$$

where p is pressure and the subscript 0 refers to the surface of the earth.

The horizontal gradient of the observed radiance in the meridional direction is

$$r_i \equiv \frac{\partial R_i}{\partial y} = \int_0^{Z_T} K_i \frac{\partial T}{\partial y}\, dZ, \tag{3}$$

where T is temperature and

$$K_i = \frac{dB_i}{dT}\frac{d\tau_i}{dZ}. \tag{4}$$

Eq. (3) shows how the horizontal radiance gradient is related to a weighted vertical integral of the horizontal temperature gradient.

The zonal component of the thermal wind in the layer bounded by the levels Z_2 and Z_1 is

$$u_t(Z_2,Z_1) = u(Z_2) - u(Z_1) = -\frac{R}{f}\int_{Z_1}^{Z_2} (\partial T/\partial y)dZ, \tag{5}$$

where R is the gas constant and f the Coriolis parameter. The thermal wind is a good approximation to the actual wind difference between two atmospheric levels as long as the wind field is close to geostrophic, as it generally is above the planetary boundary layer outside the tropics.

Comparison of Eqs. (3) and (5) shows that they both contain vertical integrals of the meridional temperature gradient; the difference between the two is that in Eq. (3) the integral is over the entire atmosphere and is weighted by K_i, whereas in Eq. (5) the integral is limited to the layer bounded by Z_2 and Z_1 and is unweighted.

If we define a function $W(Z)$ such that

$$W(Z) = \begin{cases} 1, & \text{if } Z_1 \leq Z \leq Z_2 \\ 0, & \text{otherwise,} \end{cases}$$

then Eq. (5) can be written

$$-fu_t(Z_2, Z_1)R^{-1} = \int_0^{Z_T} W \frac{\partial T}{\partial y}\, dZ. \tag{6}$$

If Eq. (3) is multiplied by coefficients c_i and summed over the N observation wavenumbers we obtain

$$\sum_{i=1}^{N} c_i r_i = \int_0^{Z_T} \left(\sum_{i=1}^{N} c_i K_i\right)(\partial T/\partial y)dZ. \tag{7}$$

Inspection of (6) and (7) indicates that if we approximate W by $\sum_{i=1}^{N} c_i K_i$, then we can estimate the thermal wind from

$$\hat{u}_t(Z_2, Z_1) = -(R/f)\sum_{i=1}^{N} c_i r_i, \tag{8}$$

where the caret indicates the estimated value. The coefficients c_i can be determined from a procedure that minimizes in some sense the difference between the approximate W-function, which we may denote by $\hat{W}$, and the actual W-function. Fig. 1 shows some actual kernel functions K_i and a typical W-function, W.

There are several different ways in which the coefficients c_i can be determined.

a. Method 1

One way is simply to minimize the form

$$J = \int_0^{Z_T} \left(\sum_{i=1}^{N} c_i K_i - W\right)^2 dz. \tag{9}$$

This procedure would minimize the difference between $\hat{W}$ and W over the entire atmosphere in a

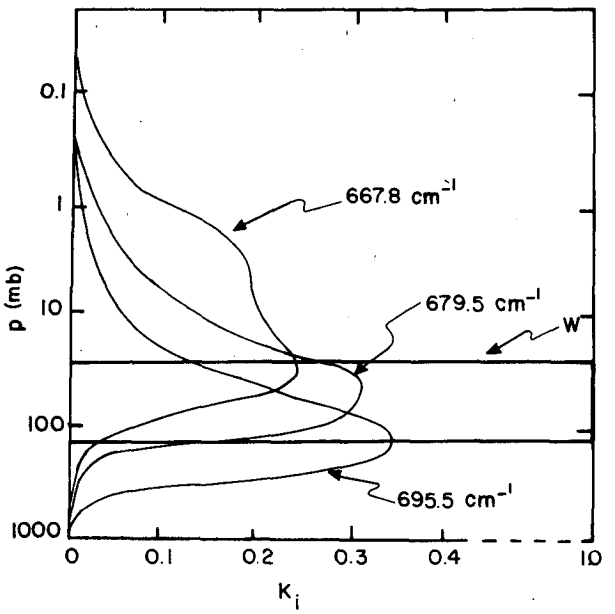

FIG. 1. K_i and W functions.

least-squares sense. The solution to this minimization problem is

$$\mathbf{c} = \mathbf{S}^{-1}\mathbf{a}, \tag{10}$$

where

$$S_{ij} = \int_0^{Z_T} K_i K_j dZ, \tag{11}$$

$$a_i = \int_{Z_1}^{Z_2} K_i dZ. \tag{12}$$

With c_i known, u_t can be determined from Eq. (8). The meridional component of the thermal wind, v_t, can be obtained with these same c_i by substituting the zonal radiance gradients $(\partial R_i/\partial x)$ for r_i in (8) and omitting the minus sign.

b. Method 2

Fleming (1979) (see also Fleming, 1972) has suggested that the coefficients c_i be determined by minimizing the quadratic form

$$J = \int_0^{Z_T} (1 - W)^2 \left(\sum_{i=1}^{N} c_i K_i - W\right)^2 dZ \tag{13}$$

subject to the unit height constraint

$$(Z_2 - Z_1)^{-1} \int_{Z_1}^{Z_2} \left(\sum_{i=1}^{N} c_i K_i\right) dZ = 1.$$

Fleming refers to the factor $(1 - W)^2$ as a penalty function that tends to sharpen up the approximate W-function, $\hat{W}$. Since $W = 1$ within the layer (Z_2, Z_1) of interest and $W = 0$ outside of this layer, Eq. (13) states that the integral of $\hat{W}$ outside the layer of interest should have a minimum value. The unit height constraint insures that the integral of $\hat{W}$ is equal to the integral of W within the layer of interest. The solution to this minimization problem is

$$\mathbf{c} = \frac{l\mathbf{S}^{-1}\mathbf{a}}{\mathbf{a}^T\mathbf{S}^{-1}\mathbf{a}}, \tag{14}$$

where

$$S_{ij} = \int_0^{Z_1} K_i K_j dZ + \int_{Z_2}^{Z_T} K_i K_j dZ \tag{15}$$

$l = Z_2 - Z_1$, and the superscript T represents the transposed vector.

c. Method 3

To determine whether there is any significant difference between the simple minimization of method 1 and the use of the penalty function as in method 2, we may use method 1 with the same unit height constraint as in method 2. Formally, the solution is the same as for method 2, i.e., Eq. (14), but with S_{ij} defined as in method 1, i.e., Eq. (11).

d. Method 4

Methods 2 and 3 both use the unit height constraint. This insures that areas such as those labeled C in Fig. 2 would cancel each other. However, the excess areas labeled A and B are undesirable and lead to inaccuracies in the solution. Fleming (1972) suggests compensating for these areas by multiply-

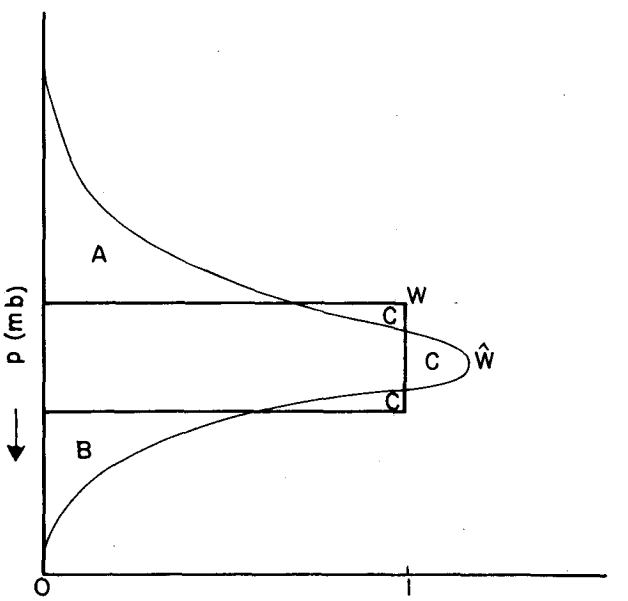

FIG. 2. Schematic W and $\hat{W}$ functions.

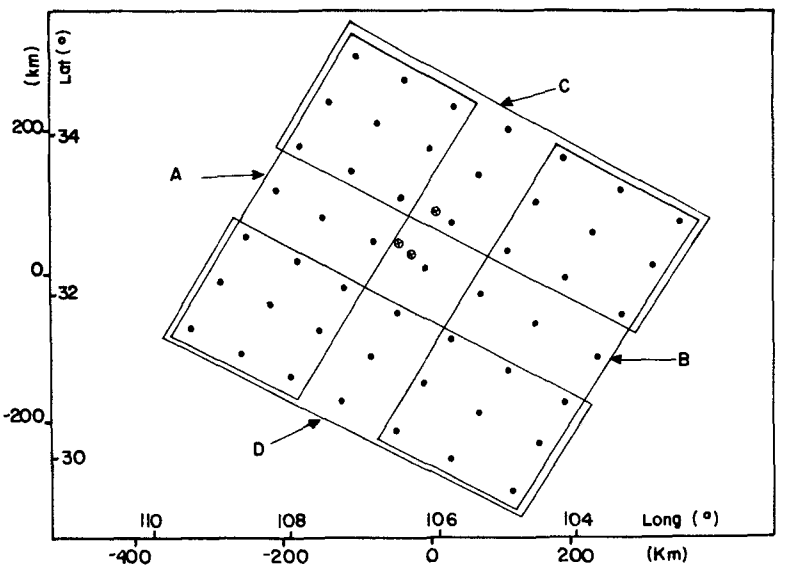

FIG. 3. Typical array of satellite radiance observation points over the White Sands area. Each dot represents the center of a spot observed by the satellite. The circled crosses show the locations of the radiosonde stations that were used for ground truth. The rectangles A, B, C and D are used in the computation of radiance gradients as explained in the text (also see Fig. 4).

ing the solution of method 2 by the factor

$$f = l\left(\int_0^{Z_T} \hat{W}dZ\right)^{-1}. \tag{16}$$

e. Method 5

To insure that the correct solution is obtained in the case where the thermal wind is not a function of altitude, i.e., the horizontal temperature gradient is constant with altitude, we may proceed as follows. We combine (5), (6) and (8) to obtain

$$\widehat{\int_{Z_1}^{Z_2} (\partial T/\partial y)dZ} = \sum_{i=1}^{N} c_i r_i = \int_0^{Z_T} \left(\sum_{i=1}^{N} c_i K_i\right)(\partial T/\partial y)dZ, \tag{17}$$

where the caret, as before, indicates the estimated value. For $(\partial T/\partial y)$ constant with altitude,

$$\widehat{(\partial T/\partial y)}(Z_2 - Z_1) = (\partial T/\partial y)\int_0^{Z_T} \left(\sum_{i=1}^{N} c_i K_i\right)dZ. \tag{18}$$

From (18) it can be seen that the estimated temperature gradient $\widehat{\partial T/\partial y}$ will equal the actual temperature gradient if

$$(Z_2 - Z_1)^{-1}\int_0^{Z_T} \left(\sum_{i=1}^{N} c_i K_i\right)dZ = 1. \tag{19}$$

This is a different form of the unit height constraint. Eq. (19) can be interpreted as stating that the vertical integral of the approximate W-function should be equal to the vertical integral of the exact W-function. This seems to be a more appropriate normalization constraint than the one given in method 2. The use of this constraint with the minimization of Eq. (9) constitutes method 5. The solution is

$$\mathbf{c} = \mathbf{S}^{-1}\mathbf{a} + \frac{l - \mathbf{b}^T\mathbf{S}^{-1}\mathbf{a}}{\mathbf{b}^T\mathbf{S}^{-1}\mathbf{b}}\mathbf{S}^{-1}\mathbf{b}, \tag{20}$$

where

$$b_i = \int_0^{Z_T} K_i dZ. \tag{21}$$

f. Traditional and regression methods

The above five methods may be called direct retrieval methods since the thermal winds are obtained directly from the radiance gradients. Using a set of colocated radiance and radiosonde data, we shall compare the results obtained from the different direct methods. We shall also compare the results of the direct methods with results obtained from method T, the traditional method, in which the thermal wind is computed from the temperatures retrieved from radiance observations, and from a linear regression method based on the relationship between the observed wind shears and the observed radiance gradients. The results obtained from the regression method represent a limiting accuracy for a particular data set for any direct linear method.

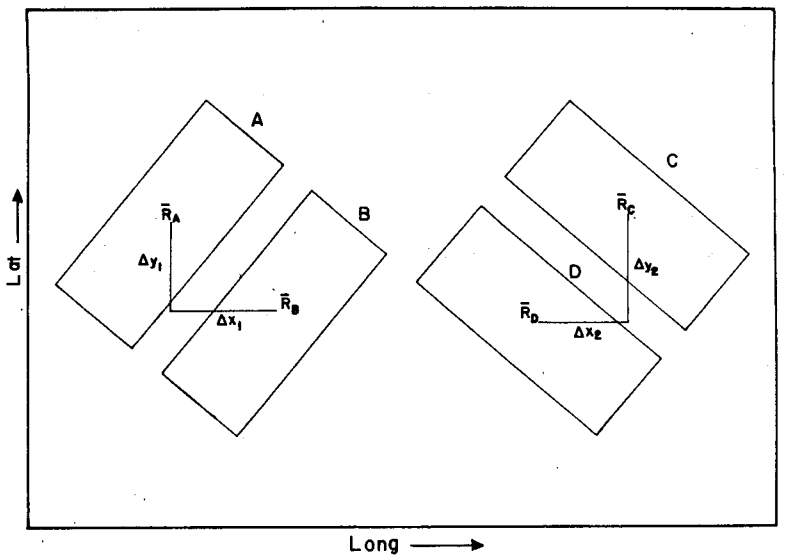

FIG. 4. Schematic diagram showing how observations from areas A, B, C and D are used to compute radiance gradients. See text.

3. Experimental details

A special series of 31 concurrent (within 1 h) sets of radiance observations from the NOAA-4 VTPR instrument and wind shear from radiosonde observations, distributed throughout one year (February to December 1975), for the White Sands Missile Range area in New Mexico (see Fig. 3), is used for evaluating the different methods. The horizontal radiance gradients over this area are estimated from a 7 × 7 slightly rectangular array of satellite radiance observations extending over an area of ~500 km on the side. The spot size (50% power contour) of each radiance observation ranges from 60 km at the subsatellite point to about 80 km at the end of each scan line. To compute the radiance gradients, four averages of 3 × 7 grid points each, as shown in Fig. 3, were made of the radiances and of the location coordinates. The radiance gradients are then obtained from application of the Taylor approximation formulas to these average values

$$\Delta R_1 = \bar{R}_A - \bar{R}_B = \frac{\partial R}{\partial x}\Delta x_1 + \frac{\partial R}{\partial y}\Delta y, \quad (22)$$

$$\Delta R_2 = \bar{R}_c - \bar{R}_d = \frac{\partial R}{\partial x}\Delta x_2 + \frac{\partial R}{\partial y}\Delta y_2, \quad (23)$$

where $\bar{R}_A$, $\bar{R}_B$, $\bar{R}_C$ and $\bar{R}_D$ are the average radiances (at a particular wavenumber) for the regions A, B, C

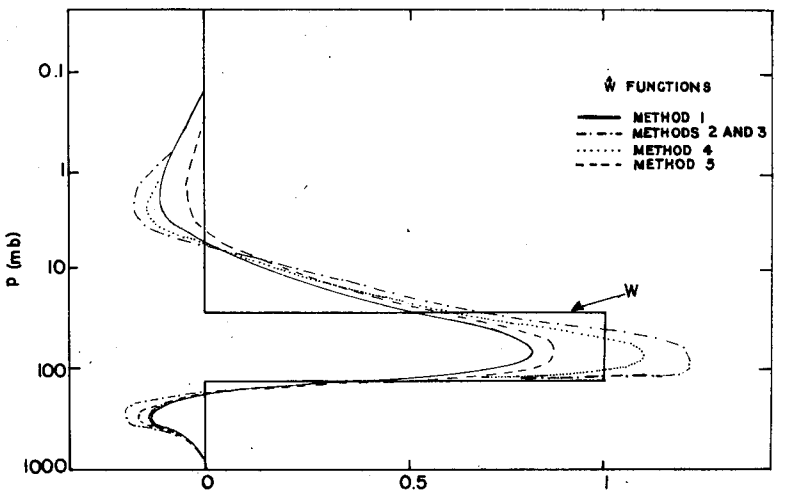

FIG. 5. Comparison of approximate ($\hat{W}$) and actual W-functions for 125–25 mb layer.

and D, as shown in Figs. 3 and 4, and Δx_1, Δy_1, Δx_2 and Δy_2 are shown geometrically in Fig. 4. These two simultaneous equations can be readily solved for the unknown radiance gradients $\partial R/\partial x$ and $\partial R/\partial y$. This simple method gave approximately the same results as a planar fit by a regression technique.

"Ground truth" was obtained from radiosonde balloons launched (nearly) simultaneously from the three stations shown in Fig. 3 about one hour prior to the overpass of the NOAA-4 satellite. The average of the three measured wind profiles was used as "truth" data for the different methods.

It was decided to compare the direct methods using just the three upper atmosphere channels (695.5, 679.5, 667.8 cm^{-1}). Sample comparisons with the use of four channels indicated no improvement in the results.

The atmospheric transmission for each of CO_2 band observing channels is assumed to be a product of the CO_2, H_2O and O_3 transmissions in that channel. A zenith angle correction to the transmissions also is included. These transmissions are computed for each case from a first-guess temperature and water vapor profile and from a standard ozone distribution.

In the traditional method, temperature retrievals are obtained with an inversion scheme similar to that of Hogan and Grossman (1972).

4. Results

Before discussing the results, it is instructive to compare the approximate W-functions of the different direct methods. Fig. 5 shows the $\hat{W}$-function for the five direct methods for the layer 125–25 mb. The $\hat{W}$-functions of methods 2 and 3 are almost identical. This suggests that there is no particular advantage to be gained by using the penalty function as in Eq. (13) rather than a straightforward minimization technique. It will be recalled that methods 2 and 3 both use the unit height constraint applied to the layer of interest. While this insures that, within the layer of interest, the area under $\hat{W}$ is equal to the area under W, it also causes greater side lobes outside the layer of interest than those of the other methods. Although method 4 also makes use of the unit height constraint in the layer of interest, the final solution coefficients are reduced by a common factor in order to reduce the side lobes, thus nullifying the intent of the unit height constraint. The $\hat{W}$ functions of the other layers have similar characteristics.

Just as the $\hat{W}$ functions of the different methods group themselves into two distinct groups—those *with* unit height constraint within the layer of interest and those *without* (included here is method 4)—so do the results. There were no substantial differences in the results obtained with methods 2 and 3, and there were no substantial differences in the results obtained with methods 1, 4 and 5. Therefore, in the discussion that follows the results of method 1 are used to represent methods 1, 4 and 5, which we may call group 1, and the results of method 2 are used to represent methods 2 and 3, which we may call group 2.

Table 1 compares the arithmetic (or systematic) errors of the group 1 and group 2 direct methods and the traditional (T) method. Also shown in the table are the observed mean wind shears. The wind shears represent the change in wind speed from the base to the top of each layer.

In general, the group 2 methods have a much greater systematic error than the group 1 methods, especially for the u component of the wind shear. The arithmetic errors of group 1 are, in general, somewhat less than those of the traditional method. The arithmetic errors of group 1 and the traditional method are small compared to the observed mean u-component wind shears, but are of the same size as the observed v-component shears, which are of the order of 1 m s^{-1} for each layer.

Table 2 shows a comparison of the root-mean-square (rms) errors of the various methods. Also included in this table are the standard errors (SE) of a linear regression method based on the relationship between the observed wind shears and observed radiance gradients. These standard errors represent

TABLE 1. Mean observed wind shears and mean arithmetic errors of wind shear retrievals (m s^{-1}). Method 1 represents the group of methods 1, 4 and 5; method 2 represents the group of methods 2 and 3; and N is the number of comparisons.

Layer		u component				v component				
			Method				Method			
(mb)	(km)	Observed	1	2	T	Observed	1	2	T	N
250–100	10.4–16.2	−8.2	6.9	7.7	2.4*	−0.4	0.7	1.0	0.0*	31
100–50	16.2–20.6	−11.6	1.9	−7.4	5.8	−1.0	0.5	0.4	1.1	31
50–20	20.6–26.5	−4.0	−1.7	−9.8	−1.6	−0.3	−0.2	−1.0	0.7	28
20–10	26.5–31.1	1.2	−0.2	4.1	−3.4	1.1	−0.7	−0.9	−0.7	15
125–25	14.8–25.0	−19.8	3.4	−1.9	7.9	−2.1	1.3	1.0	2.3	31

* Values for Method T are for the 300–100 mb layer (9.6–16.2 km).

TABLE 2. Root-mean-square errors, standard error of regression technique (SE), and standard deviation of observations of wind shear (σ) (m s^{-1}). Method 1 represents the group of methods 1, 4 and 5; method 2 represents the group of methods 2 and 3, and N is the number of comparisons.

Layer		u component					v component					
		Method					Method					
(mb)	(km)	1	2	T	SE	σ	1	2	T	SE	σ	N
250–100	10.4–16.2	12.	14	7.6*	7.7	10.1	11.	14	8.3*	7.3	11.7	31
100–50	16.2–20.6	6.8	14	7.9	4.9	5.0	6.5	11	3.5	3.5	4.7	31
50–20	20.6–26.5	8.0	22	5.2	5.5	7.0	8.0	18	4.4	3.5	3.5	28
20–10	26.5–31.1	5.8	35	6.3	4.9	7.3	4.5	19	2.5	2.4	2.1	15
Mean		8.2	21	6.8	5.8	7.4	7.5	16	4.7	4.2	5.5	
125–25	14.8–25.0	8.7	10	10.1	6.4	9.4	12.	15	5.5	5.5	8.0	31

* Values for method T are for the 300–100 mb layer (9.6–16.2 km).

estimates of the minimum rms errors that can be achieved by any direct linear retrieval method. In addition, the table includes the standard deviations (σ) of the observed wind shears.

Inspection of Table 2 reveals that the rms errors of group 2 are typically more than twice as large as those of group 1, the mean rms errors for the four layers between 250 and 10 mb being 21 and 8 m s^{-1}, respectively, for the u component, and 15.5 and 7.5 m s^{-1} for the v component.

A comparison of group 1 rms errors with those of the traditional method shows that they are about the same magnitude for u-component but greater for group 1 for the v component. However, for neither method does the rms error go much below the standard deviation of the observations. This implies that the error obtained by assuming that the wind shear is always equal to the observed climatological value at White Sands would be no greater than that obtained when satellite observations are used to estimate the wind shears.

Comparison of the rms errors of the direct methods and the standard errors of the regression technique shows that the difference between the two is larger for the v component of the wind shear than for the u-component.

In both Tables 1 and 2, a separate row of results is presented for the 125–25 mb layer. This layer is approximately twice as large as the other layers, and it was thought that, in view of the "resolving power" difficulties of the basic radiance observations, the results might be improved for such a "thick" layer. However, inspection of the tables indicates that there is no particular reduction in the errors for this thicker layer.

5. Conclusions and discussion

Several methods have been derived for determination of thermal winds directly from the horizontal gradients of satellite radiance observations. These methods are intercompared using a special series of satellite VTPR radiance and radiosonde wind observations over the White Sands Proving Ground area in the United States. The direct methods are also compared to the "traditional" method, in which thermal winds are computed from the horizontal temperature gradients obtained from temperature profiles retrieved from the satellite radiance observations, and to a linear regression method.

Of the direct methods tested, those that do not apply the unit height constraint to the layer of interest give the best results. The use of the unit height constraint causes larger side lobes in the $\hat{W}$-function, thus introducing more undesirable information from the region outside the layer of interest than in the case of the methods that have no such constraint.

There appears to be no particular advantage to introducing a penalty function $(1 - W)^2$ into the integral form that is minimized to obtain the solution coefficients for the direct methods.

The best direct methods gave results comparable to those obtained with the traditional method. However, all the methods examined are not particularly skillful at retrieving the wind shears from the radiance observations. This lack of skill is probably associated with a number of factors.

We believe that the major factor leading to lack of skill is the error associated with trying to evaluate a relatively small horizontal gradient over a relatively small horizontal distance. For the geographical region and atmospheric layers studied in this research, typical u-component wind shears are of the order of 10 m s^{-1}. Such wind shears imply, through the thermal wind equation, meridional temperature gradients of about 3.5°C (1000 km)$^{-1}$. Differentation of the Planck function with respect to temperature indicates that for the temperatures and wavenumbers of concern here, a change of 1°C is approximately equivalent to a change of one radiance unit (mW m^{-2} sr^{-1} cm). Thus, the observed wind shears are associated with radiance gradients that are of the order of 3.5 radiance units for 1000 km. However,

in the present investigation these radiance gradients are estimated from radiance observations over characteristic horizontal distances of ~300 km—which means radiance differences of about 1 radiance unit or temperature differences of ~1°C must be measured. The VTPR instruments had characteristic sensitivities of 0.25 radiance units (even larger at 667.8 cm^{-1}), a significant fraction of the radiance differences that had to be measured in order to retrieve the observed thermal winds. Thus, the VTPR instruments are just not sensitive enough to measure the small horizontal radiance differences over distances of ~300 km associated with typical meridional temperature gradients in the stratosphere over White Sands. The situation for the v-component is even worse, since typical v-component wind shears are less than those of the u-component.

Other factors contributing to errors in the retrievals include the differences between the actual and the approximate W-functions, uncertainties in transmission functions, and possible differences between the thermal wind shear and the actual wind shear.

The above discussion leads us to suggest that much better results might be obtained by applying the direct methods of the group 1 type to regions of the atmosphere with typically greater wind shears than those encountered in the stratosphere over White Sands and/or to characteristic horizontal distances greater than the 300 km used in the present study. Improved instrumentation in the current generation of satellite sounding equipment should also lead to improved retrievals.

Acknowledgment. The research reported herein has been sponsored in part by the United States Army through its European Research Office.

REFERENCES

Fleming, H. E., 1972: A method for calculating atmospheric thickness directly from satellite radiation observations. *Preprints. Conf. Atmospheric Radiation*, Fort Collins, Amer. Meteor. Soc., 134–137.

——, 1979: Determination of vertical wind shear from linear combinations of satellite radiance gradients: A theoretical study. U.S. Naval Postgraduate School Rep. NPS63-79-004, 42 pp. [Available from Defense Documentation Center, Cameron Station, Alexandria, VA 22314].

Grody, N. C., C. M. Hayden, W. C. C. Shen, P. W. Rosekranz and D. H. Staelin, 1979: Typhoon June winds estimated from scanning microwave spectrometer measurements at 55.45 GHz. *J. Geophys. Res.*, **84**, 3689–3695.

Hogan, J. S., and K. Grossman, 1972: Test of a procedure for inserting satellite radiance measurements into a numerical circulation model. *J. Atmos. Sci.*, **29**, 797–800.

Zak, J. Allen, and H. A. Panofsky, 1968: Estimation of stratospheric flow from satellite 15-micron radiation. *J. Appl. Meteor.*, **7**, 136–140.